



Toxic effects of ammonia and thermal stress on the intestinal microbiota and transcriptomic and metabolomic responses of *Litopenaeus vannamei*



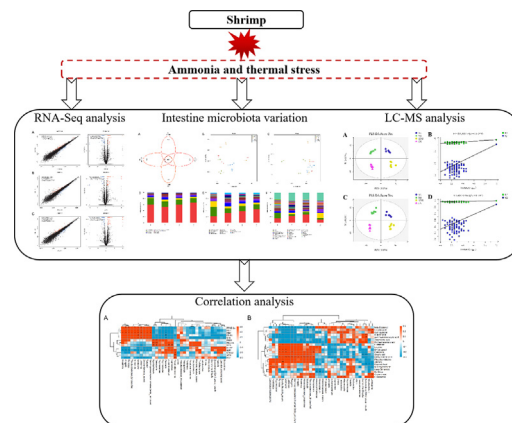
Yafei Duan, Dalin Xiong, Yun Wang, Hua Li, Hongbiao Dong, Jiasong Zhang *

Key Laboratory of South China Sea Fishery Resources Exploitation & Utilization, Ministry of Agriculture and Rural Affairs, Guangdong Provincial Key Laboratory of Fishery Ecology and Environment, South China Sea Fisheries Research Institute, Chinese Academy of Fishery Sciences, Guangzhou 510300, PR China

HIGHLIGHTS

- Intestinal microbiota and immune molecules, and haemolymph metabolism were disrupted.
- Intestinal Firmicutes abundance was increased but Bacteroidetes abundances was decreased.
- Intestinal peritrophic membrane and antimicrobial genes were differentially expressed.
- Haemolymph amino acid and arachidonic acid metabolism were disturbed.
- Several stress-related gene and metabolite markers were identified.

GRAPHICAL ABSTRACT



ARTICLE INFO

Article history:

Received 23 April 2020

Received in revised form 17 August 2020

Accepted 19 August 2020

Available online 21 August 2020

Editor: Daniel Wunderlin

Keywords:

Ammonia
Intestine microbiota
Metabolome
Shrimp
Temperature
Transcriptome

ABSTRACT

Ammonia and thermal stress frequently have harmful effects on aquatic animals. The intestine is an important barrier allowing the body to defend against stress. In this study, we investigated the intestinal microbiota and transcriptomic and metabolomic responses of *Litopenaeus vannamei* subjected to individual and combined ammonia and thermal stress. The results showed that obvious variation in the intestinal microbiota was observed after stress exposure, with increased levels of Firmicutes and decreased levels of Bacteroidetes and Planctomycetes. Several genera of putatively beneficial bacteria (*Demequina*, *Weissella* and *Bacteroides*) were abundant, while *Formosa*, *Kriegella*, *Ruegeria*, *Rhodopirellula* and *Lutimonas* were decreased; pathogenic bacteria of the genus *Vibrio* were increased under individual stress but decreased under combined stress. The intestinal transcriptome revealed several immune-related differentially expressed genes associated with the peritrophic membrane and antimicrobial processes in contrasting accessions. Haemolymph metabolomic analysis showed that stress exposure disturbed the metabolic processes of the shrimp, especially amino acid metabolism. This study provides insight into the underlying mechanisms associated with the intestinal microbiota, immunity and metabolism of *L. vannamei* in response to ammonia and thermal stress; ten stress-related metabolite markers were identified, including L-lactic acid, gulonic acid, docosahexaenoic acid, L-lysine, gamma-aminobutyric acid, methylmalonic acid, trans-cinnamate, N-acetylserotonin, adenine, and dihydrouracil.

© 2020 Published by Elsevier B.V.

* Corresponding author at: South China Sea Fisheries Research Institute, Chinese Academy of Fishery Sciences, 231 Xingangxi Road, Guangzhou 510300, PR China.
E-mail address: jiasongzhang@hotmail.com (J. Zhang).

1. Introduction

Pacific white shrimp (*Litopenaeus vannamei*) is an important aquatic economic species and a high-quality protein source for humans. Shrimp live their entire life in water; therefore, they are inevitably affected by environmental pollutants (Liu and Chen, 2004). Ammonia is a common pollutant in aquatic environments and is mainly produced by the decomposition of organic wastes, including faeces and excess feed. In intensive culture ponds, the concentration of ammonia can increase as high as 46 mg/L (Chen et al., 1988). Ammonia stress affects shrimp health and causes high mortality, immune disorders, and susceptibility to disease (Cheng and Chen, 2002; Jiang et al., 2004; Liu and Chen, 2004; Zhang et al., 2012). Additionally, habitat water temperature drives all biological processes of aquatic animals, including physiological and behavioural processes (Pörtner and Knust, 2007). In subtropical climate regions, especially summer, the water temperature of shrimp ponds often exceeds 34 °C (Preston et al., 1995; Jackson and Wang, 1998; You et al., 2010). Elevated temperatures can also induce stress responses and cause physiological discomfort in shrimp (Hewitt and Duncan, 2001; Wang and Chen, 2006). It has been reported that ammonia concentration is affected by water temperature, and the toxicity of ammonia to aquatic animals increases with increased water temperature (Kir et al., 2004). However, the physiological response mechanism of shrimp under the combined stress of elevated ammonia and temperature is still unclear.

The intestine is one of the tissues with the most contact between organisms and the external environment, and it is also the largest immune organ. The intestine provides a barrier for host health that is composed of intestinal mucosa and a stable functional microbiota (Duan et al., 2018a). The intestinal barrier not only plays an important role in maintaining the stability of the internal environment but also can effectively prevent the invasion of pathogen-derived substances and the displacement of bacterial endotoxins (Gao et al., 2016). A stable functional microbiota contributes to host health, including nutritional, metabolic and immune homeostasis, and metabolic function; conversely, microbiota imbalance will impair host health and increase disease susceptibility (Hsiao et al., 2013; Koeth et al., 2013). In particular, the intestinal microbiota co-metabolizes with its host, and the microbiota and host immune system can exchange metabolites between the intestinal lumen and mucosal surfaces, as well as the systemic circulation (Gentile and Weir, 2018; Zimmermann et al., 2019). Beneficial microbial metabolites will promote host health, while harmful microbial metabolites can lead to host disease (Levy et al., 2017). Thus, the interaction between the intestinal microbiota and the immunity and metabolism of the host has a profound effect on host health.

In previous studies, we confirmed that, individually, ammonia and thermal stress caused intestinal mucosal damage and immune disruption in *L. vannamei*, and ammonia stress also induced intestinal microbiota alterations (Duan et al., 2018a, 2018b); however, the underlying molecular mechanisms are unknown. Therefore, in this study, we investigated the individual and combined effects of ammonia and thermal stress on the intestinal microbiota community of *L. vannamei*. Then, transcriptomics and metabolomics were used to analyse the changes in intestinal immune factors and haemolymph metabolites, respectively, and the association between variations in intestinal microbes and host immune factors and metabolites was also analysed.

2. Materials and methods

2.1. Shrimp and rearing conditions

Healthy *L. vannamei* with an average body weight of 6.7 ± 0.5 g were randomly obtained from a local farming pond in Shenzhen Base, South China Sea Fisheries Research Institute, Chinese Academy of Fishery Sciences (Shenzhen, China). The shrimp were acclimated in sand-filtered and aerated seawater (salinity 30‰, pH 8.4, temperature 30 °C) for

7 days before the stress experiment. Commercial feed was provided to the shrimp daily at 5% of their body weight three times per day (07:00, 12:00, 18:00). Two-thirds of the water was exchanged per day.

2.2. Stress exposure and sample collection

After 7 days of acclimation, the healthy shrimp in the intermoult stage were divided into four groups: the control group (CG), the thermal stress group (TG), the ammonia stress group (AG), and the combined ammonia and thermal stress group (ATG). Each group included three replicate tanks. The shrimp were housed at 50 individuals per tank, and each tank contained 100 L of aerated seawater. According to previous studies, the 72 h 50% lethal concentration (LC50) values of ammonia-N for *L. vannamei* juveniles were 32.15, 43.17 and 44.93 mg/L at salinities of 15, 25 and 35, respectively (Lin and Chen, 2001). Increasing the water temperature from 30 °C to 33 °C could affect the intestinal health of *L. vannamei* (Duan et al., 2018b). Based on the pre-experiment results, we set the ammonia concentration and thermal stress temperature of this study as 15 mg/L and 33 °C, respectively, and sampled at 72 h.

In detail, the CG tanks were filled with seawater, the water temperature was kept at 30 °C and ammonia was kept at 0 mg/L; the TG tanks were filled with seawater, the water temperature was kept at 33 °C and ammonia was kept at 0 mg/L; the AG tanks were filled with seawater, the water temperature was kept at 30 °C and ammonia was kept at 15 mg/L; the ATG tanks were filled with seawater, the water temperature was kept at 33 °C and ammonia was kept at 15 mg/L. All the groups had the same culture conditions except that the ammonia-N concentrations and water temperatures were different. The ammonia-N concentration of the AG and ATG was maintained at 15.0 mg/L by adding NH₄Cl solution to the seawater. The concentration of ammonia in the seawater was adjusted in time to ensure stability. The water temperature stability of all the groups was continuously maintained using aquarium heaters. The tanks used in the stress exposure stage were the same as those used in the acclimation stage, and the shrimp were not moved to new tanks. The stress exposure lasted for 72 h.

After 72 h of exposure, the intestines (without faeces) and haemolymph of the shrimp from each tank were sampled individually. In detail, six shrimp intestines from each tank were mixed for microbial community analysis, and six shrimp intestines from each tank were mixed for transcriptome analysis; these 12 shrimp haemolymphs were mixed for metabolomic analysis. Overall, each group contained 3 duplicate microbial samples, 3 duplicate transcriptome samples, and 6 duplicate metabolome samples. All the samples were snap-frozen in liquid nitrogen until experimental analysis.

2.3. Intestinal microbiome analysis

Total genomic DNA of the microbes from the intestine samples was extracted using the TAB/SDS method, and then the V4 region of the bacterial 16S rDNA gene was amplified using a pair of barcoded fusion primers, 515F (5'-GTGCCAGCMGCCGCGG-3') and 806R (5'-GGAC TACHVGGGTWCTAAT-3'). The PCRs were carried out using Phusion® High-Fidelity PCR Master Mix (New England Biolabs). The PCR products were mixed in equidensity ratios and purified. Then, sequencing libraries were constructed using the NEBNext® Ultra™ DNA Library Prep Kit for Illumina (NEB, USA) and sequenced on an Illumina MiSeq platform.

Paired-end reads were merged using FLASH and assigned to each sample according to the unique barcodes. Sequence analysis was performed by UPARSE software, and the operational taxonomy units (OTUs) were defined with $\geq 97\%$ similarity (Edgar, 2013). Chimeric sequences were determined by UCHIME (Edgar et al., 2011). Alpha diversity was calculated with three metrics, including Chao1, Simpson, and Shannon index, using Mothur software (Schloss et al., 2011). A Venn diagram was used to count the number of unique and shared OTUs in multiple samples. Beta diversity was evaluated by principal coordinates

analysis (PCoA) plots based on weighted and unweighted UniFrac metrics using the package Ape. Differential intestinal bacteria of TG vs CG, AG vs CG, and ATG vs CG were identified. Microbial composition was analysed at the phylum, class and genus levels. Linear discriminant analysis (LDA) effect size (LEfSe) analysis was performed using the Python LEfSe package (Segata et al., 2011) to identify differential bacterial taxa within different groups. RandomForest analyses were performed based on Kyoto Encyclopedia of Genes and Genomes (KEGG) level 3 using the R randomForest package. A Cytoscape network was constructed to analyse the correlations and differences between microbial communities based on OTU abundance using Cytoscape software (<http://www.cytoscape.org/>). All statistical analyses were conducted using R package software. In addition, the alpha diversity index values were expressed as the mean \pm SE and analysed using two-way ANOVA (SPSS ver 20.0), followed by Tukey's multiple comparison tests to analyse the significant differences between independent experimental groups and treatments. $P < 0.05$ was regarded as statistically significant.

2.4. Intestinal transcriptome analysis

Total RNA was extracted from the intestine using TRIzol® Reagent (Invitrogen, USA), and genomic DNA was removed using DNase I (TaKaRa, China). A high-quality RNA sample (1 μ g) was used to construct a sequencing library using a TruSeq™ RNA sample preparation kit from Illumina (San Diego, CA). After quantification by TBS380, paired-end libraries were sequenced with the Illumina HiSeq PE 2 \times 151 bp read length. Raw paired-end reads were trimmed, and the clean reads were screened using Trimmomatic software (<http://www.usadellab.org/cms/uploads/supplementary/Trimmomatic>). Then, all the clean reads were separately aligned to the *L. vannamei* genome with orientation mode using TopHat software (<http://tophat.cbcb.umd.edu/>). Differentially expressed genes (DEGs) of TG vs CG, AG vs CG, and ATG vs CG were identified, and the expression level of each transcript was calculated according to the reads per kilobase of exon per million mapped reads (RPKM) method. Cuffdiff (<http://cufflinks.cbcb.umd.edu/>) was used for differential expression analysis. The DEGs between two samples were selected using the following criteria: logarithmic fold change >2 and false discovery rate (FDR) <0.05 . The GO functional enrichment of the DEGs was analysed using Goatools software (<https://github.com/tanghaibao/Goatools>). KEGG pathway analysis of the DEGs was performed using KOBAS software (<http://kobas.cbi.pku.edu.cn/home.do>). The statistical analyses of the GO and KEGG enrichment were set as Bonferroni-corrected P -values <0.05 .

2.5. Haemolymph metabolomics analysis

Six haemolymph sample replicates of shrimp from each group were used for metabolomics analysis. All the haemolymph samples were taken from liquid nitrogen and thawed in the refrigerator at 4 °C, and metabolite extraction was performed using methanol and 2-chlorobenzalanine. Twenty microlitres of each sample was taken for quality control (QC), and the rest was used for LC-MS detection. Liquid chromatography was accomplished in a Thermo Ultimate 3000 system equipped with an ACQUITY UPLC® HSS T3 (150 \times 2.1 mm, 1.8 μ m,

Waters) column. Mass spectrometry was executed on a Thermo Q Exactive mass spectrometer. Data-dependent acquisition (DDA) MS/MS experiments were performed with HCD scans. Dynamic exclusion was implemented to remove some unnecessary information in the MS/MS spectra.

The original data were converted into mzXML format (xcms input file format) through Proteowizard software (v3.0.8789). The R (v3.3.2) XCMS package was used for the identification, filtration and alignment of peaks. Base peak chromatograms (BPCs) were obtained through continuous description of the ions with the highest intensity in each mass spectrogram. All the data were determined using quality control (QC) and quality assurance (QA). After standardized treatment by autoscaling with mean-centering and scaling to unit variance (UV), partial least squares-discriminant analysis (PLS-DA) of the metabolomics data was performed using the R language ropls package. All the metabolites were classified according to KEGG and Metabolon.inc. Differential metabolites (DMs) of TG vs CG, AG vs CG, and ATG vs CG were identified. Based on the exact mass match (error < 15 ppm) and secondary spectra MS/MS, metabolite identification was performed by searching Metlin (<http://metlin.scripps.edu/>), MoNA (<https://mona.fiehnlab.ucdavis.edu/>) and company databases (BioNovoGene, China). Agglomerate hierarchical clustering of the DMs was performed using the R software (v3.3.2) pheatmap package. The DMs were annotated with KEGG pathway analysis using metaboanalyst software (www.metaboanalyst.ca). The PLS-DA model was used to determine the DMs between the pairwise comparison groups with the first principal component of variable importance in projection (VIP) values (VIP ≥ 1) combined with a P -value ≤ 0.05 .

2.6. Correlation analysis of intestinal bacteria and the DEGs and DMs

Pearson correlation analysis was employed to reveal the correlation between intestinal bacteria and the intestinal immune-related DEGs of the host and haemolymph DMs using the Cytoscape software coNet plug-in, and the correlation coefficient and P -value threshold were not set. $P < 0.05$ was regarded as statistically significant, $P < 0.01$ was regarded as very significant, and $P < 0.001$ was regarded as extremely significant. A heatmap was used to show the correlation of intestinal bacteria with genes and metabolites respectively.

3. Results

3.1. Intestinal microbiota changes

3.1.1. Richness and diversity

A total of 772,926 clean reads were obtained from all the microbial samples, and the average number of clean reads per sample was 64,410. A rarefaction curve analysis of the observed species per sample was sufficient (Fig. S1). Compared with the CG, the Chao index of the three stress groups was increased, the Simpson index of the TG and AG was also increased, but the Shannon index was not significantly changed (Table 1); the unique OTUs of the three stress groups were increased, and those of the ATG were lower than those of the TG and AG (Fig. 1A). PCoA of weighted and unweighted UniFrac distances was

Table 1
Alpha diversity of intestinal microbial of *L. vannamei* after ammonia and thermal stress.

Group	Observed	Chao1	Shannon	Simpson	Coverage (%)
CG	961 \pm 363	1225 \pm 322 ^a	3.77 \pm 0.78	0.0843 \pm 0.0361 ^a	99.61
TG	1510 \pm 113	1723 \pm 194 ^b	3.98 \pm 1.26	0.1668 \pm 0.0284 ^b	99.54
AG	1660 \pm 289	1968 \pm 271 ^b	3.82 \pm 1.80	0.2187 \pm 0.0317 ^b	99.40
ATG	1531 \pm 273	1786 \pm 216 ^b	4.16 \pm 0.38	0.0886 \pm 0.0272 ^a	99.36

Values represent the mean \pm SE ($n = 3$). The different letters (a, b, c) indicate significant differences ($P < 0.05$) among groups.

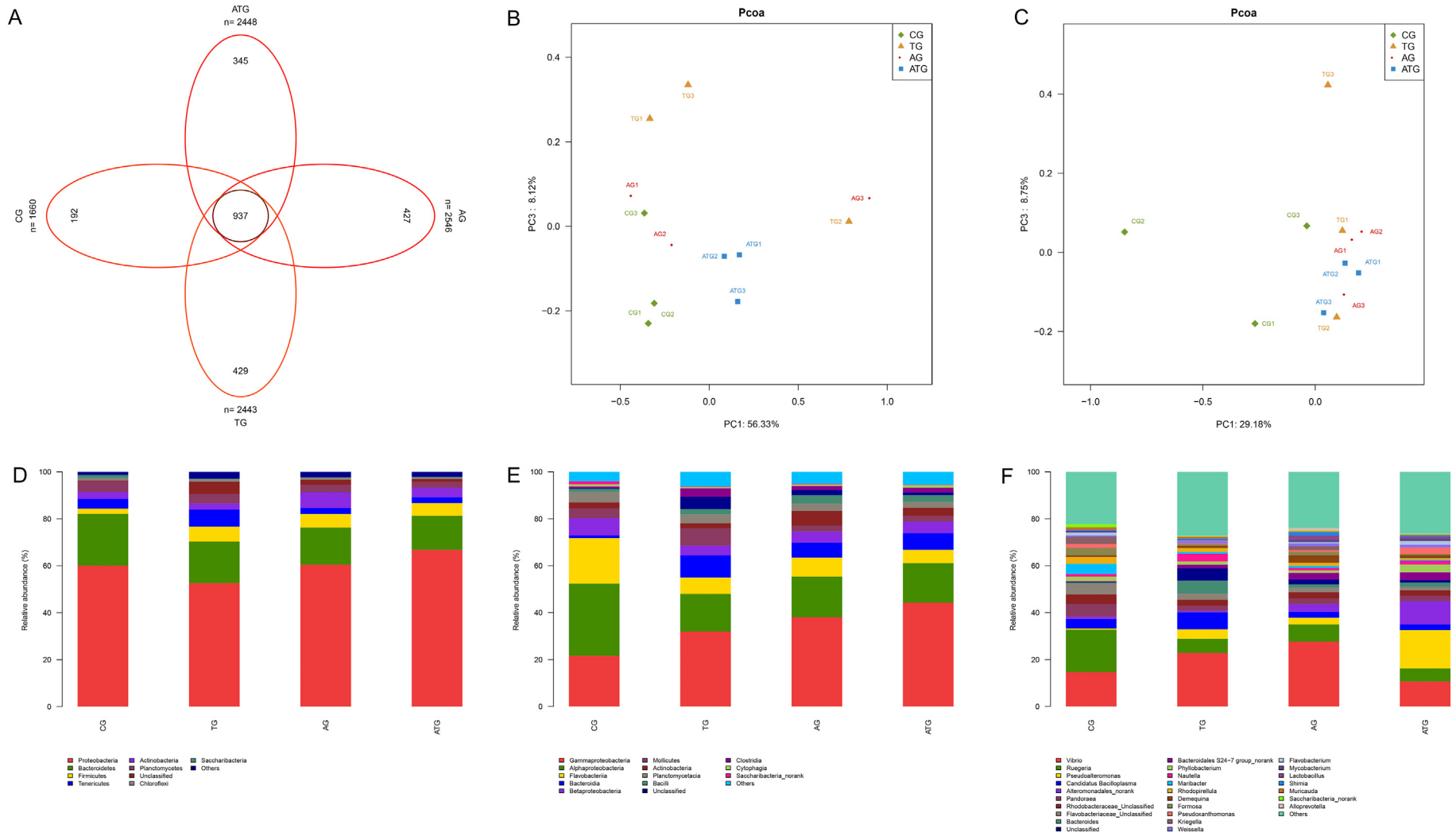


Fig. 1. Intestinal microbial diversity and composition of *L. vannamei* after ammonia and thermal stress. The number of unique and shared OTUs between different treatments indicated by the Venn diagram (A). PCoA plots based on weighted UniFrac metrics (B) and unweighted UniFrac metrics (C). Average relative abundances of dominant bacterial phyla (D), classes (E) and genera (F) in the intestine of tadpoles under different treatments.

further performed to confirm that the intestinal bacteria in the CG and the three stress groups were clearly separated (Fig. 1B, C).

3.1.2. Intestinal microbial composition

The taxa of dominant bacteria among the three groups were similar, while their abundance was altered. At the phylum level, compared with the CG, the relative abundance of Proteobacteria was decreased in the TG but increased in the ATG; the relative abundance of Bacteroidetes was decreased in the three stress groups, but the abundance of Firmicutes was increased (Fig. 1D). At the class level, the relative abundance of Alphaproteobacteria, Flavobacteriia, Betaproteobacteria and Planctomycetacia decreased in the three stress groups, but the abundance of Gammaproteobacteria, Bacteroidia and Bacilli increased (Fig. 1E). Differences were also observed at the genus level: certain genera, such as *Bacteroides*, *Demequina*, and *Weissella*, were increased in the three stress groups, but *Formosa*, *Kriegella*, *Lutimonas*, *Muricauda*, *Pandoraea*, *Rhodopirellula*, and *Ruegeria* were decreased. In addition, *Vibrio* was increased in the TG and AG but decreased in the ATG (Fig. 1F).

3.1.3. Changes in the intestinal bacterial phylotypes

LEfSe was employed to analyse the differential abundances of bacterial taxa in the four groups. In the cladogram, Rickettsiales contributed to the CG, while Lactobacillaceae contributed to the AG (Fig. 2A). In the LEfSe LDA, the abundances of 1, 1, 4 and 3 bacterial taxa were enriched in the CG, TG, AG and ATG, respectively. Specifically, Rickettsiales was enriched in the CG, *Butyrivibrio* was enriched in the TG, *Lactobacillus* and *Alloprevotella* were enriched in the AG, and *Tenacibaculum* and *Propionigenium* were enriched in the ATG (Fig. 2B). Network analyses further confirmed the differences in the microbiota. Based on the Cytoscape network analysis of relative phylum abundance, the most dominant OTUs, OTU2 and OTU3, both belonged to Proteobacteria, and the OTUs of Bacteroidetes had the highest correlation with those of Firmicutes (Fig. 2C). Network branching diagrams were used to further analyse the differences in the microbiota in the four groups, and only *Lactobacillus* was significantly dominant in the AG (Fig. 2D). The prediction function of the intestinal microbiota was analysed using PICRUSt. Based on random forest KEGG classification, compared with those in the CG, “pathogenic *Escherichia coli* infection” and “regulation of actin cytoskeleton” were both increased in the three stress groups, but “biosynthesis and biodegradation of secondary metabolites”, “pertussis”, and “bladder cancer” were all decreased (Fig. 2E).

3.2. Intestinal transcriptome analysis

3.2.1. Identification and functional annotation of the DEGs

RNA-Seq analysis of the *L. vannamei* intestine from the four groups generated 545,434,190 total raw reads and 81,815,128,500 raw bases, with 515,505,124 total clean reads and 76,872,591,171 clean bases produced after optimization and quality control; the clean reads ratio was 93.04%–94.67%. Then, the clean reads were mapped to the *L. vannamei* genome, and the mapped rate was 80.76%–86.52% (Table S1). All raw reads were submitted to the Sequence Read Archive (SRA) (accession: PRJNA626527).

A total of 334 DEGs were identified in the intestines in the three stress groups compared with the CG (Fig. S2), and 13 DEGs were present in all groups, including FK506-binding protein 4 (FKBP), carbohydrate sulfotransferase 11, titin, mannose-binding protein (MBP), chitinase 4 precursor (Chit-4p), and peritrophin-1 (PT-1) (Table S2). Specifically, the TG contained 74 upregulated and 78 downregulated genes, the AG contained 74 upregulated and 55 downregulated genes, and the ATG contained 66 upregulated and 79 downregulated genes (Fig. 3).

The DEGs were annotated by GO enrichment analysis. The dominant GO terms of the TG, AG and ATG were basically similar. Of these, “single-organism process”, “metabolic process” and “cellular process” were the dominant subcategories in biological processes; “cell”, “cell part” and

“organelle” were the dominant subcategories in cellular components; and “catalytic activity” and “binding” were the dominant subcategories in molecular functions (Fig. 4A–C).

All the DEGs were further analysed by KEGG pathway analysis. Compared with the CG, the most enriched pathways of the TG were “ABC transporters”, “caffeine metabolism”, and “vitamin digestion and absorption” (Fig. 4D); those of the AG were “DNA replication”, “histidine metabolism”, “alanine, aspartate and glutamate metabolism”, and “ascorbate and aldarate metabolism” (Fig. 4E); and those of the ATG were “prion diseases”, “linoleic acid metabolism” and “ABC transporters” (Fig. 4F).

3.2.2. Identification of the immune-related DEGs

Several immune-related DEGs were identified based on the NR database annotations, which provided a better understanding of the immune response of the *L. vannamei* intestine induced by stresses. Specifically, 13 immune-related DEGs were mainly shared by the three stress groups. Of these, 4 DEGs, including FKBP, MBP, PT-1, and Chit-4p, were present in the three comparisons of TG vs CG, AG vs CG, and ATG vs CG; 4 DEGs including prophenoloxidase-activating enzyme 2 α (PPAE-2 α), alpha 2 macroglobulin (α 2M), haemocyte homeostasis-associated protein (HHAP), and aminopeptidase N (APN), were present in the two comparisons of TG vs CG and ATG vs CG; 5 DEGs, including haemolymph clottable protein (HCP), peritrophin-55 (PT-55), chitinase (Chit), mucin-3A (Muc-3A), and serine proteinase inhibitor 8 (SPI8), were present in the two comparisons of AG vs CG and ATG vs CG (Table 2).

3.3. Haemolymph metabolome analysis

3.3.1. Multivariate analysis of the metabolite profiles

Metabolomic analysis was conducted to explore the alterations in haemolymph metabolic profiles after stresses. The metabolic profiles of the haemolymph of *L. vannamei* among the different groups by LC-MS analysis are shown in Fig. S3. The PLS-DA score plot and permutation test further showed a significant difference among the four groups in both positive and negative ionization modes (Fig. 5), suggesting that ammonia and thermal stress caused metabolic phenotype alterations in shrimp haemolymph. A total of 338 metabolites were identified in the shrimp haemolymph using MS/MS analysis, and the largest category was “amino acids, peptides, and analogues” (37.1%), followed by “carbohydrates and carbohydrate conjugates” (15.9%) and “fatty acids and conjugates” (15.2%) (Fig. S4).

3.3.2. Identification and functional annotation of the DMs

We further screened the DMs between the control and the three stress groups. Compared with the CG, the TG contained 42 upregulated and 20 downregulated DMs, the AG contained 44 upregulated and 31 downregulated DMs, and the ATG contained 34 upregulated and 35 downregulated DMs (Fig. 6B, 6D, 6F). To explore the potential metabolic pathways affected by stresses, all the DMs were further analysed by KEGG annotation. Compared with the CG, the most enriched pathways in the TG were “phenylalanine metabolism”, “phenylalanine, tyrosine and tryptophan biosynthesis”, “alanine; aspartate and glutamate metabolism”, and “arachidonic acid metabolism” (Fig. 6A); those in the AG were “histidine metabolism”, “vitamin B6 metabolism”, “valine, leucine and isoleucine biosynthesis” (Fig. 6C); and those in the ATG were “D-glutamine and D-glutamate metabolism”, “beta-alanine metabolism”, “alanine, aspartate and glutamate metabolism”, and “arachidonic acid metabolism” (Fig. 6E).

Certain DMs related to organism health, including gamma-aminobutyric acid (GABA), L-lactic acid, gulonic acid, and docosahexaenoic acid, were all increased in the three stress groups, but L-lysine, methylmalonic acid, adenine, dihydrouracil, and N-acetylserotonin were all decreased. Additionally, trans-cinnamate was increased in the TG but decreased in the AG and ATG; beta-

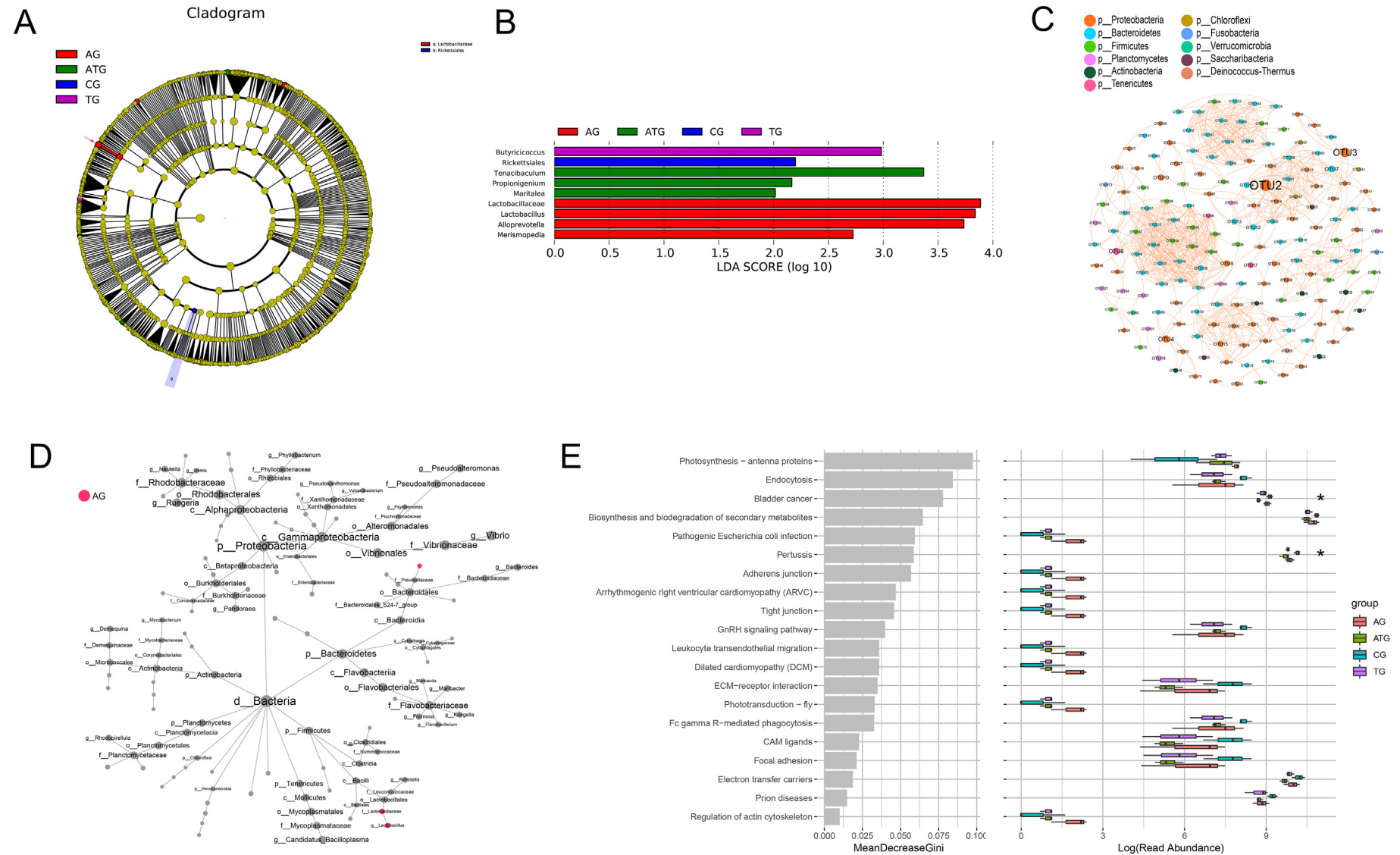


Fig. 2. Intergroup variation, network and metabolism analyses of the intestinal microbes of *L. vannamei* after ammonia and thermal stress. (A) LEfSe cladogram. (B) LDA score of LEfSe-PICRUST. (C) Relevance network analyses based on the bacterial phylum level. The nodes represent the phylum classification of the OTUs, and the node size indicates the relative abundance of each taxon. The nodes representing the same phylum are shown in the same colour. Lines between two OTUs represent the correlation. (D) Differential network analyses. The nodes represent the species classification, and the node size indicates the relative abundance. The node colour provides information about the difference; black indicates no significant difference, and the remaining colours indicate significant differences in the corresponding group. The names of taxa with an abundance above 1% are provided. (E) Microbial metabolism prediction based on KEGG pathway analysis. *Indicates a significant difference ($P < 0.05$) among groups. (For interpretation of the references to colour in this figure legend, the reader is referred to the web version of this article.)

sitosterol was increased in the AG and ATG, but ergocalciferol, L-histidine and phosphorylcholine were decreased; arachidonic acid and glyceric acid were increased in the TG and ATG; hydroquinone,

L-isoleucine and DL-dopa were increased in the TG and AG, but pyridoxine was decreased; while stearic acid was only decreased in the TG (Table 3).

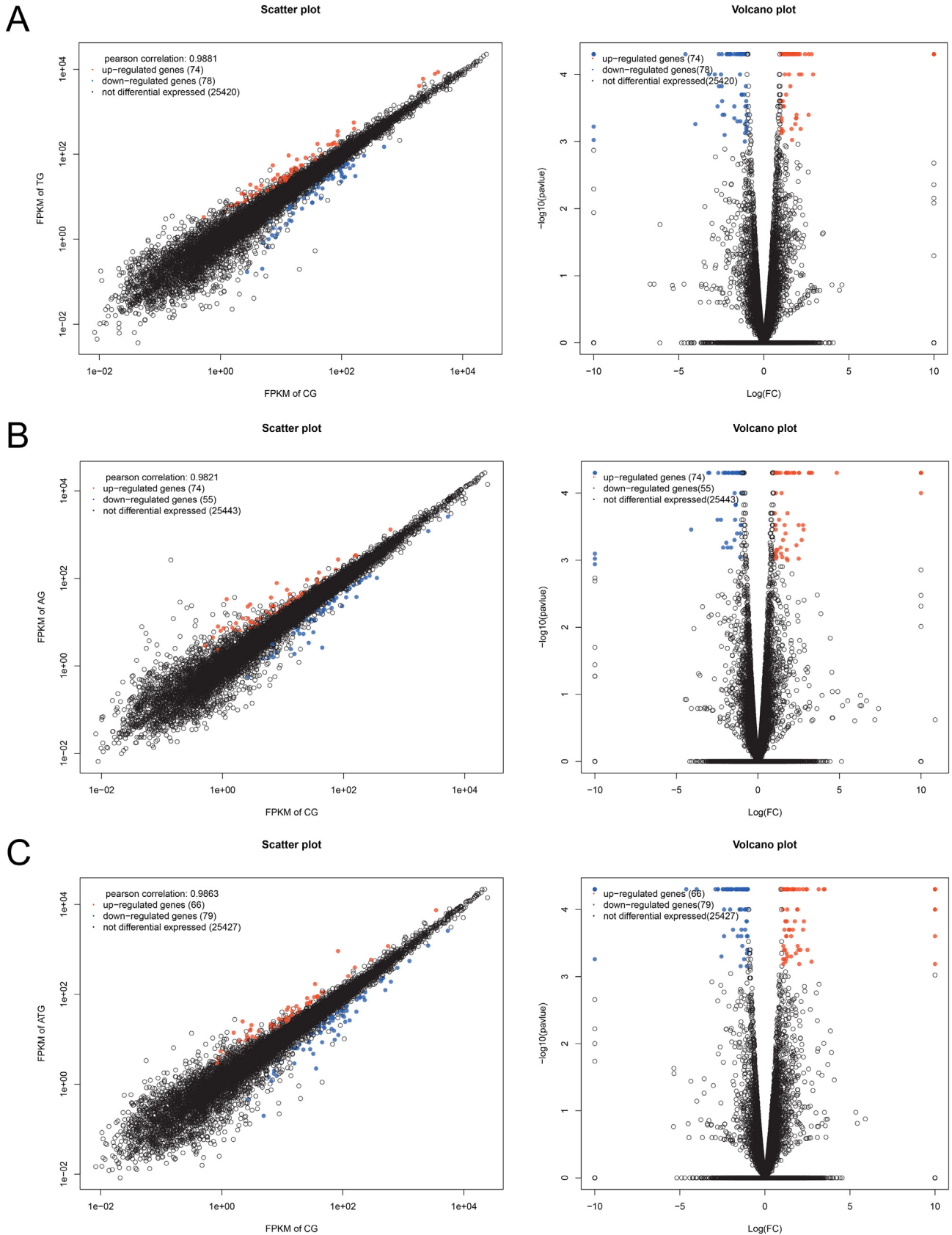


Fig. 3. Scatter and volcano plots of the DEGs in the intestine of *L. vannamei* after ammonia and temperature stress. (A) TG vs CG. (B) AG vs CG. (C) ATG vs CG.

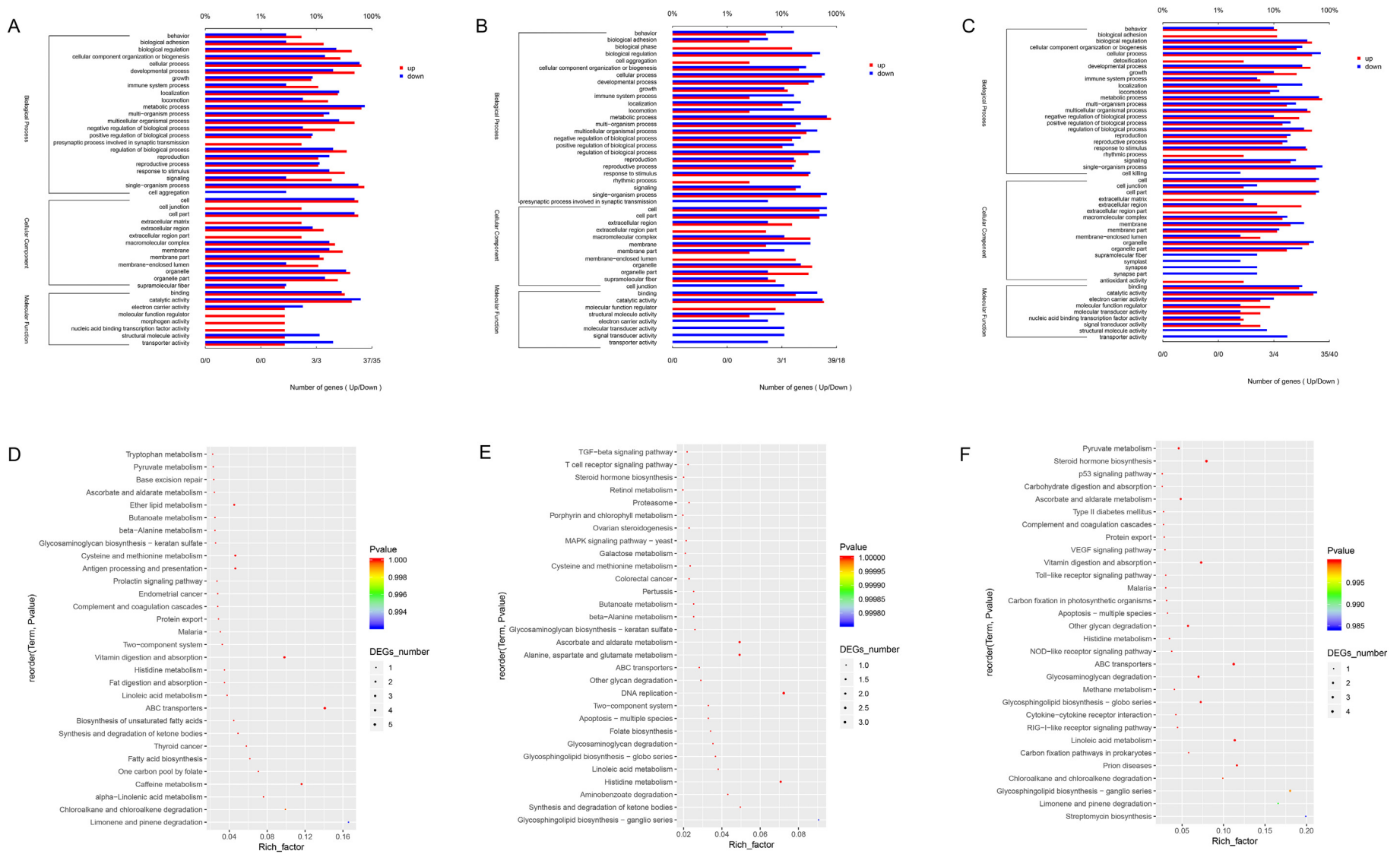


Fig. 4. The most enriched GO terms and pathways of the DEGs in the intestine of *L. vannamei* after ammonia and thermal stress. (A) GO terms of TG vs CG. (B) GO terms of AG vs CG. (C) GO terms of ATG vs CG. (D) KEGG pathways of TG vs CG. (E) KEGG pathways of AG vs CG. (F) KEGG pathways of ATG vs CG.

Table 2

Transcription profiles of the immune related DEGs in intestinal of *L. vannamei* after ammonia and thermal stress.

Gene id	Function annotation	TG vs CG	AG vs CG	ATG vs CG
LVAN21979	Peritrophin-1 (PT-1)	Down	Down	Down
LVAN21973	Peritrophin-55 (PT-55)	N/A	Down	Down
LVAN08663	Mucin-3A (Muc-3A)	N/A	Up	Up
LVAN00179	FK506-binding protein 4 (FKBP)	Down	Down	Down
LVAN14100	Aminopeptidase N (APN)	Up	N/A	Up
LVAN20408	Hemolymph clottable protein (HCP)	N/A	Up	Up
LVAN12988	Hemocyte homeostasis-associated protein (HHAP)	Up	N/A	Up
LVAN02632	Prophenoloxidase-activating enzyme 2a (PPAE-2α)	Down	N/A	Down
LVAN12835	Alpha 2 macroglobulin (α2M)	Up	N/A	Up
LVAN10203	Serine proteinase inhibitor 8 (SPI8)	N/A	Up	Up
LVAN17073	Mannose-binding protein (MBP)	Down	Down	Down
LVAN18516	Chitinase 4 precursor (Chit-4p)	Up	Up	Up
LVAN00215	Chitinase (Chit)	N/A	Down	Down

3.4. Association between the intestinal microbiota and host immune factors and metabolites

To reveal the relationships between intestinal microbial and immune and metabolite parameters, heat maps were generated by Pearson correlation analysis. In the correlation between intestinal bacterial and host immune DEGs, *Maribacter*, *Kriegella*, *Formosa*, *Muricauda*, and

Lutimonas were positively correlated with changes in the *PT-1*, *PPAE-2α* and *MBP* genes; *Mycobacterium* and *Demequina* were positively correlated with changes in the *Muc-3A*, *FKBP* and *SPI8* genes; *Ruegeria* was positively correlated with changes in the *PT-1* and *MBP* genes; *Bacteroides* was positively correlated with changes in the *HHAP* gene; and *Pseudoxanthomonas* was positively correlated with changes in the *APN*, *HCP* and *Chit-4p* genes (Fig. 7A). In the correlation between intestinal bacterial and host metabolites, *Demequina* was positively correlated with changes in glyceric acid and L-lactic acid; *Bacteroides* was positively correlated with changes in arachidonic acid; and *Lutimonas*, *Muricauda*, *Rhodopirellula*, and *Ruegeria* were positively correlated with changes in methylmalonic acid but negatively correlated with changes in beta-sitosterol (Fig. 7B).

4. Discussion

4.1. Intestinal microbiota in response to ammonia and thermal stress

Environmental pollutants and challenging environments have adverse effects on the intestinal barrier function of aquatic animals (Duan et al., 2018a; Tinkov et al., 2018; Qiao et al., 2019). In this study, ammonia and thermal stress altered the intestinal microbial composition of *L. vannamei*, notably, Proteobacteria, Bacteroidetes and Firmicutes were the dominant intestinal bacteria of *L. vannamei*. Proteobacteria are frequently prominent in the intestinal microbiome of shrimp (Fan et al., 2019; Holt et al., 2020) and participate in carbon complexes and nitrogen degradation (Cottrell and Kirchman, 2000;

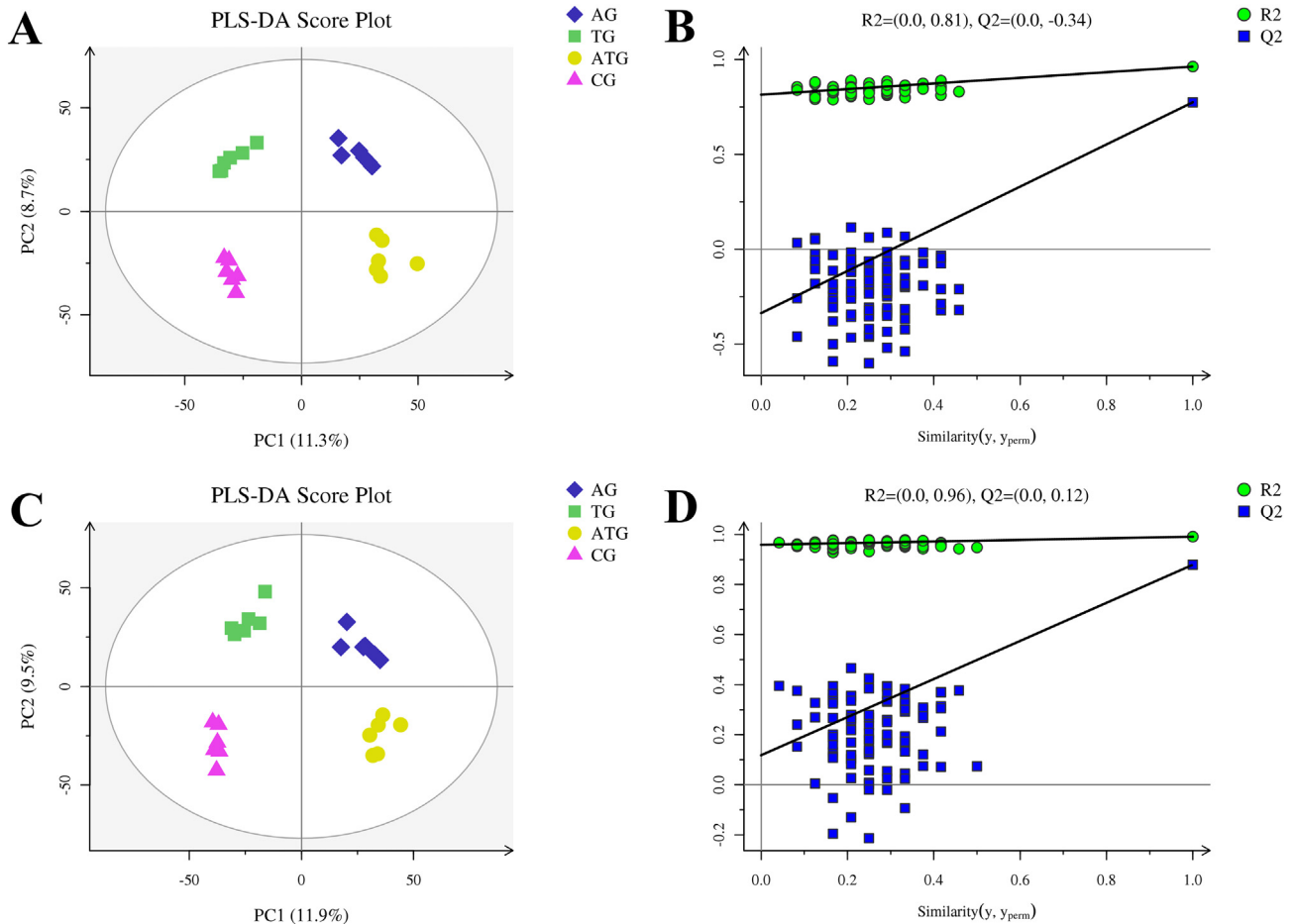


Fig. 5. Derived PLS-DA score plots and corresponding permutation testing of PLS-DA from the LC-MS metabolite profiles in the haemolymph of *L. vannamei* after ammonia and thermal stress. (A) PLS-DA score plot of positive ions. (B) Permutation testing of positive ions. (C) PLS-DA score plot of negative ions. (D) Permutation testing of negative ions.

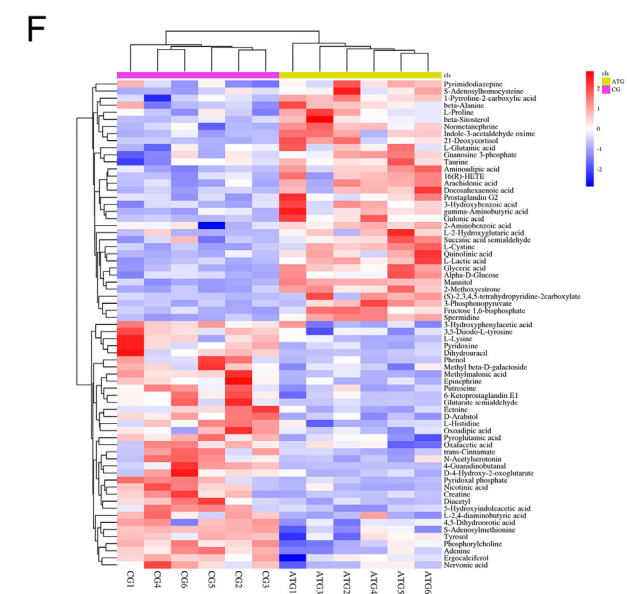
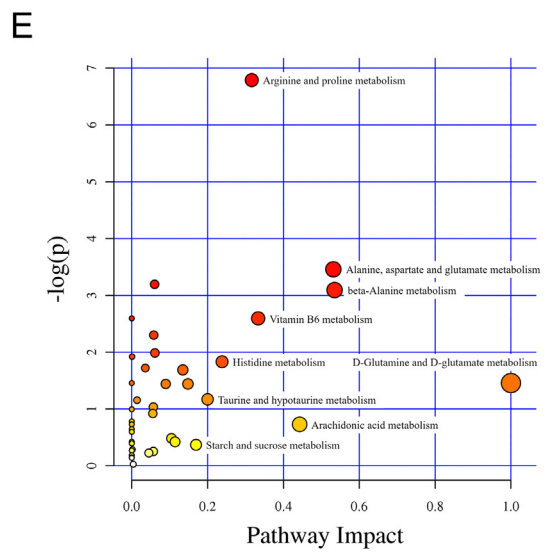
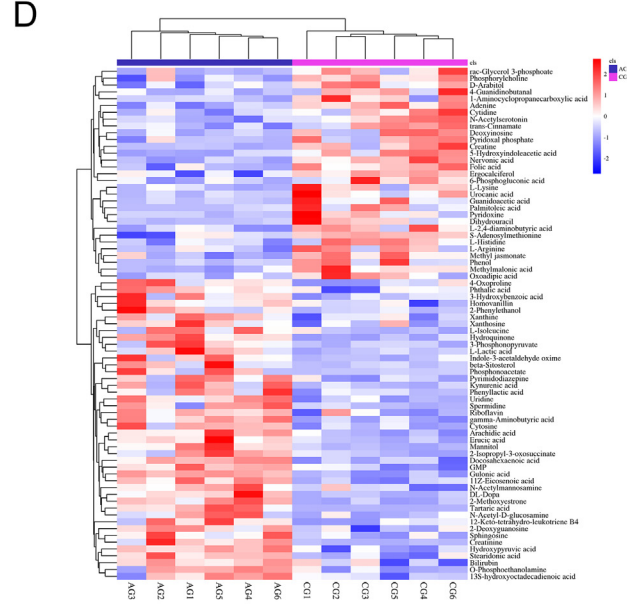
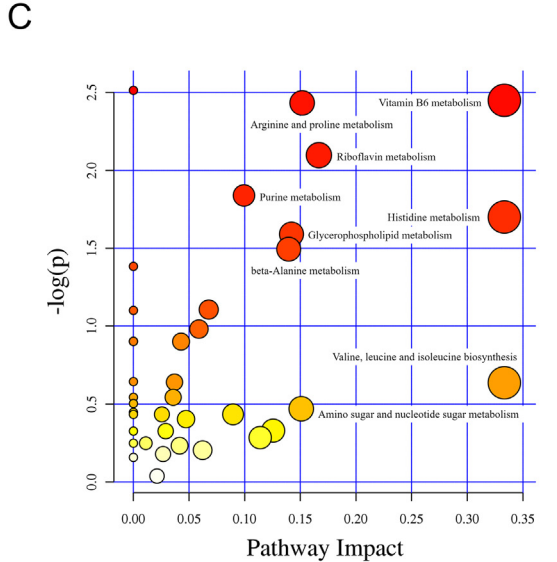
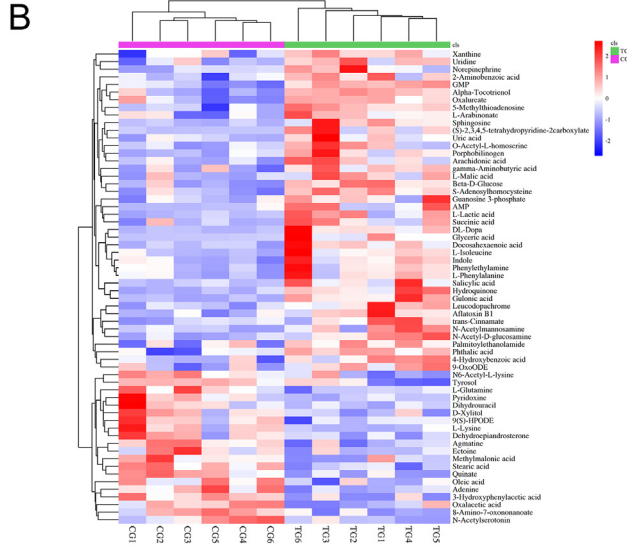
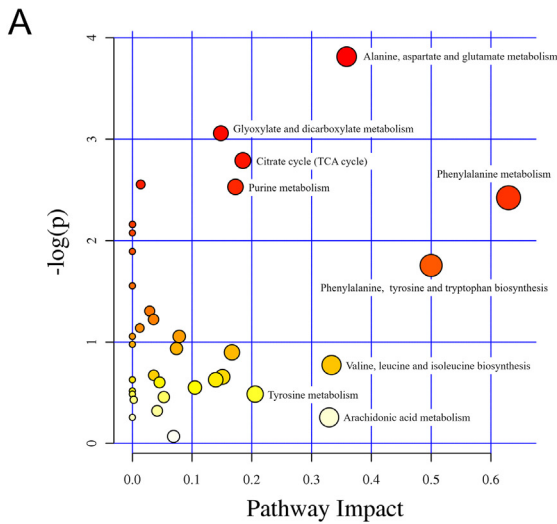


Table 3
Significantly changed DMs in haemolymph of *L. vannamei* after ammonia and thermal stress.

Metabolites name	Log2 fold change			Categories
	TG vs CG	AG vs CG	ATG vs CG	
Glyceric acid	3.40	/	1.69	Carbohydrate
L-Lactic acid	0.67	0.57	0.60	Carbohydrate
Gulonic acid	0.67	0.57	0.60	Carbohydrate
Arachidonic acid	1.06	/	1.17	Lipid
Stearic acid	-0.56	/	/	Lipid
Docosahexaenoic acid	1.28	0.97	1.32	Lipid
beta-Sitosterol	/	2.47	2.00	Lipid
Ergocalciferol	/	-0.75	-0.61	Lipid
Phosphorylcholine	/	-0.60	-0.64	Lipid
L-Isoleucine	1.54	1.33	/	Amino acid
L-Lysine	-1.60	-1.53	-1.33	Amino acid
L-Histidine	/	-0.27	-0.31	Amino acid
Gamma-aminobutyric acid	0.32	0.75	0.70	Amino acid
Methylmalonic acid	-1.25	-1.88	-2.25	Amino acid
trans-Cinnamate	0.98	-1.28	-1.15	Amino acid
DL-Dopa	2.21	1.55	/	Amino acid
N-acetylserotonin	-0.13	-0.19	-0.13	Amino acid
Adenine	-0.38	-0.66	-0.75	Nucleotide
Dihydrouracil	-1.64	-2.80	-2.80	Nucleotide
Hydroquinone	2.82	2.61	/	Xenobiotics
Pyridoxine	-0.71	-0.61	/	Cofactors and vitamins

Klase et al., 2019). In this study, the changes in abundance of Proteobacteria suggested that ammonia and thermal stress had different effects on Proteobacteria homeostasis; among them, thermal stress might decrease the contribution of Proteobacteria to host metabolism and digestion, while the combined stress induced their functions. Bacteroides and Firmicutes both participate in fermentation and provide nutrients to the host (Gilliland et al., 2012; Wexler, 2007); Bacteroidetes can promote energy metabolism by increasing carbohydrate metabolism (Shin et al., 2015), while Firmicutes facilitate energy harvest by improving lipid metabolism (Turnbaugh et al., 2008; O'Sullivan et al., 2002). The increased abundance of Firmicutes and the decreased abundance of Bacteroides indicated that ammonia and thermal stress might affect the ability of *L. vannamei* intestinal bacteria to metabolize nutrients.

At the genus level, several dominant genera exhibited obvious differences among groups. Among them, we were primarily interested in host health-related bacteria. *Vibrio* is a major pathogen that can cause severe economic loss in shrimp farming (Soto-Rodriguez et al., 2015). Hence, the increase in *Vibrio* abundance indicated that ammonia and thermal stress induced a proportion of pathogenic bacteria in the shrimp intestine and potentially increased the risk of disease. *Ruegeria* can degrade phosphate triesters, which are synthesized organophosphorus compounds that exist in plasticizers and pesticides (Achbergerová and Nahálka, 2014; Yamaguchi et al., 2016). *Rhodopirellula* can help facilitate global carbon and nitrogen cycling by breaking down substantial amounts of organic material, such as "marine snow", including aggregates of zooplankton, phytoplankton and protists (Klindworth et al., 2014). *Lutimonas* is a strictly aerobic heterotrophic nitrifying bacterium that degrades ammonia (Fu et al., 2009). The decrease in the abundance of *Ruegeria*, *Rhodopirellula* and *Lutimonas* indicated that ammonia and thermal stress could potentially affect the metabolism of organic material, ammonia, and phospholipids. *Demequina* can produce α -amylase to degrade starch into glucose and dextrin (Wei et al., 2018). *Weissella* is a lactic acid bacterium that can

synthesize beneficial substances such as synthetic bacterin, oligosaccharides and exopolysaccharides (Park et al., 2013; Lynch et al., 2014). *Bacteroides* can produce carbohydrate metabolism-related enzymes, vitamins, glycans, and cofactor enzymes to promote food digestion (Karlsson et al., 2011). Thus, we speculated that the increased abundance of *Demequina*, *Weissella* and *Bacteroides* in the intestine of *L. vannamei* could provide more nutrition and beneficial substances to the host as an adaptation to these stresses. *Alloprevotella* can ferment carbohydrates to produce acetic acid and succinic acid (Downes et al., 2013). In this study, the enriched abundance of *Alloprevotella* might provide protection for intestinal mucosa in response to ammonia stress.

4.2. Intestinal transcriptomic response to ammonia and thermal stress

In this study, we used RNA-Seq technology to analyse the effect of ammonia and thermal stress on the intestinal transcriptome in *L. vannamei*. Based on the analysis of KEGG pathways, the individual and combined ammonia and thermal stress had different effects on gene expression in the intestine. For example, individual thermal stress mainly affected ABC transporters, caffeine metabolism, and the digestion and absorption of vitamins; individual ammonia stress mainly affected the metabolism of amino acids (histidine, alanine, aspartate and glutamate), ascorbate and aldarate; and combined thermal and ammonia stress mainly influenced ABC transporters and linoleic acid metabolism. ABC transporters are multifunctional transmembrane proteins that play important roles in the regulation of cell osmotic pressure, detoxification metabolism and immune response (Jaskulak et al., 2020). Furthermore, thermal stress affected intestinal vitamin homeostasis, ammonia stress affected gut protein homeostasis, and combined stress affects intestinal energy storage and supply. Vitamins are trace substances that maintain normal physiological functions (Nguyen et al., 2012). Amino acids and lipids are important components and energy sources for the organisms (Lee et al., 2018). Therefore, our data suggests that thermal and ammonia stresses have caused a dysfunction of shrimp intestinal metabolic functions, which may potentially affect its important role in host's immune response.

Intestinal immunity is an important line of defence for organisms against foreign invaders. The peritrophic membrane (PM) is an effective barrier of the shrimp intestinal epithelium that prevents foreign substance invasion. Peritrophin (PT) is an important component of the peritrophic membrane (PM) (Du et al., 2006). Muc-3A is a glycoprotein component of intestinal mucus that can resist pathogen attachment and invasion (Ogata et al., 2017). In this study, the expression of *PT-1* and *PT-55* was downregulated, while that of *Muc-3A* was upregulated, indicating that ammonia and thermal stress might affect the integrity of the PM and that the mucus was induced in the organism to maintain intestinal homeostasis. The FKBP family is responsible for the quality control of protein processing (Galat, 1993), which contributes to physiological homeostasis and environmental adaptation in *Artemia* (Maniatsi et al., 2015); FKBP46 of *P. monodon* could co-interact with the WSSV viral protein VP15 during virion assembly (Sangsuriya et al., 2011). APN is a membrane-bound enzyme that can influence immune and inflammatory responses by regulating local chemokine concentrations (Kanayama et al., 1995; Proost et al., 2007). Thus, the downregulated expression of *FKBP* and the upregulated expression of *APN* revealed that immune and inflammatory responses were induced in the shrimp intestine.

Foreign substances can enter the circulatory system of the organism through the damaged intestine. The organism can rely on its haemolymph coagulation and immune molecules to prevent pathogen invasion. HCP is an important component in haemolymph coagulation

Fig. 6. The most enriched KEGG pathways and hierarchical clustering analysis of the DMs in the haemolymph of *L. vannamei* after ammonia and thermal stress. The enriched pathway (A) and hierarchical clustering (B) of TG vs CG. The enriched pathway (C) and hierarchical clustering (D) of AG vs CG. The enriched pathway (E) and hierarchical clustering (F) of ATG vs CG.

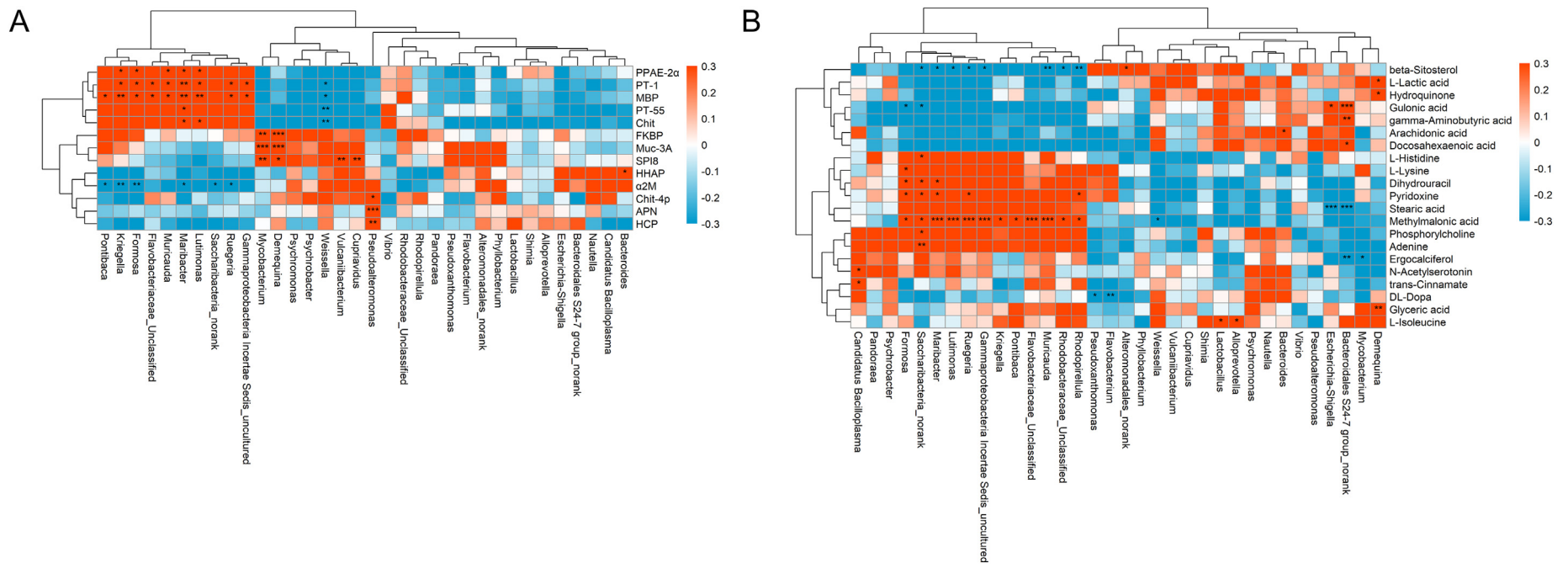


Fig. 7. Significant correlation between intestinal bacteria at the genus level and DEGs and DMs. (A) The correlation of intestinal bacteria and immune-related DEGs. (B) The correlation of intestinal bacteria and DMs. The correlation coefficient is represented by different colours (red, positive correlation; blue, negative correlation). *Represents significantly negative or positive correlations ($P < 0.05$; $**P < 0.01$; $***P < 0.001$). (For interpretation of the references to colour in this figure legend, the reader is referred to the web version of this article.)

(Cheng et al., 2008). HHAP can regulate haemocyte homeostasis by inhibiting apoptosis in shrimp (Apitanyasai et al., 2015). Thus, we speculated that the upregulated expression of *CP* and *HHAP* would facilitate the haemolymph coagulation process to resist stress. The prophenoloxidase (proPO) system is an important component in shrimp immunity. Of this system, *PPAE* catalyses proPO as an active phenoloxidase (PO), and *SPI* and $\alpha 2M$ can regulate the proPO system by inhibiting serine protease (SP) activity (Khorattanakulchai et al., 2017). As a lectin, *MBP* can activate the complement system by binding specific SP (Argayosa et al., 2011). Chitin in crustacean intestines can help digest food and control pathogens that contain chitin (Mali et al., 2004; Zhou et al., 2018). In this study, the expression of *SPI8* and $\alpha 2M$ was up-regulated, while the expression of *PPAE-2 α* , *MBP* and *Chit* was down-regulated, suggesting that ammonia and thermal stress might disrupt the proPO system in shrimp intestine, thereby affecting the antibacterial process of shrimp.

4.3. Haemolymph metabolomics in response to ammonia and thermal stress

Haemolymph metabolomics analysis further proved that ammonia and thermal stress affected the metabolic function of *L. vannamei*, especially amino acid metabolism. Interestingly, in the most enriched pathway, individual thermal stress mainly affected “phenylalanine metabolism” and “phenylalanine, tyrosine and tryptophan biosynthesis”, individual ammonia stress mainly affected “histidine metabolism” and “valine, leucine and isoleucine biosynthesis”, and the combined stress mainly affected “D-glutamine and D-glutamate metabolism”. Hence, we speculated that organisms utilized different metabolic adaptation strategies for different stresses. Pyridoxine (VB6) is a component of some coenzymes in the body and participates in amino acid metabolism (Giri et al., 1997). In this study, the decreased level of VB6 further confirmed that these stresses caused the disorder of amino acid metabolism.

Lysine is a limiting amino acid that participates in protein synthesis; it can also participate in lipid metabolism as a substrate for carnitine (Harpaz, 2005). In this study, the decreased level of L-lysine indicated that lipid metabolism might also be altered by stresses. Lipid metabolism provides essential fatty acids and energy for organisms and plays important roles in the immune response of aquatic animals to environmental stress (Lee et al., 2018). In this study, the arachidonic acid metabolism pathway was altered in the TG and ATG, and the level of arachidonic acid was increased. In addition, the level of docosahexaenoic acids was also increased in the three stress groups. Arachidonic (20:4n-6) and docosahexaenoic acids (22:6n-3) are both long-chain polyunsaturated fatty acids that have beneficial effects on the immunity of aquatic animals (Aguilar et al., 2012; Ding et al., 2018; Zhang et al., 2019). Therefore, we speculated that the increased level of these fatty acids was a strategy for shrimp to cope with stress.

We further identified several differential metabolites related to the health of the organism, and they fluctuated in all three stresses. Lactic acid is the product of anaerobic metabolism in animals, and previous studies have shown that the lactic acid content in fish blood increases after stress (Currey et al., 2013). In this study, the increased level of L-lactic acid indicated that stress-induced anaerobic metabolism was enhanced in shrimp. *N*-acetylserotonin is a precursor of melatonin and is an indole amine-type hormone that can be used as a free radical scavenger to reduce stress-induced lipid peroxidation (Stuss et al., 2010). GABA is an important neurotransmitter that can improve the antioxidative status and stress tolerance of aquatic animals (Xie et al., 2015; Wu et al., 2016). Gulonic acid is an important intermediate in the production of vitamin C, which can act as an effective nutrient and antioxidant (Yang et al., 2017). In this study, the decreased level of *N*-acetylserotonin and the increased level of gulonic acid and GABA indicated that these components might facilitate the antioxidant response to stress. Methylmalonic acid can be converted into succinic acid

under the catalysis of enzymes and vitamin B12 and participate in the citric acid cycle. In this study, the decreased level of methylmalonic acid indicated that the citric acid cycle was affected by these stresses. Adenosine is a basic component of nucleic acids, and it is also involved in cellular respiration and the synthesis energy substances, such as adenosine triphosphate (ATP), coenzyme nicotinamide adenine dinucleotide (NAD) and flavin adenine dinucleotide (FAD). Uracil is a unique base component of RNA that can be catalysed by dihydropyrimidine dehydrogenase (DPD) to dihydrouracil. In this study, the decreased levels of adenosine and uracil indicated that the production of energy and nucleic acid substances were affected by these stresses. Therefore, individual and combined ammonia and thermal stress disordered the metabolic homeostasis of shrimp, including energy substances and antioxidants.

4.4. Correlation between intestinal microbial changes and host health

Intestinal microbiota variation is closely related to host health, which will cause host immune and metabolic disorders and increase disease susceptibility (Levy et al., 2017). In this study, the decreased levels of *Formosa*, *Kriegella*, *Ruegeria*, *Muricauda* and *Lutimonas* were positively correlated with changes in shrimp intestinal immune-related genes (*PT-1*, *PPAE-2 α* and *MBP*) and methylmalonic acid, indicating that these bacteria might affect the immunity and citric acid cycle of *L. vannamei*. *Formosa* participate in the depolymerization of seaweed polysaccharides (Dogs et al., 2017; Silchenko et al., 2018). *Kriegella* has the ability to produce acid from galactose, lactose and melibiose (Nedashkovskaya et al., 2008). Thus, the decreased levels of *Formosa* and *Kriegella* suggested that ammonia and thermal stress might influence the carbohydrate metabolism of intestinal bacteria. As beneficial substance-producing bacteria, the increased level of *Bacteroides* was positively correlated with the changes in the *HHAP* gene and arachidonic acid, indicating that *Bacteroides* was involved in the immune response and arachidonic acid metabolism of *L. vannamei* to ammonia and thermal stress. As a starch-degrading bacteria, the increased level of *Demequina* was positively correlated with the changes in immune-related genes (*PT-1*, *PPAE-2 α* and *MBP*) and glycolytic metabolites (glyceric acid and L-lactic acid), indicating that *Demequina* was involved in the immune response and glycolysis of *L. vannamei* to ammonia and thermal stress. Several of the highly relevant bacteria, genes and metabolites selected in this study might be used as biomarkers for shrimp in response to ammonia and thermal stress.

5. Conclusions

We investigated the toxic effects of ammonia and thermal stress on *L. vannamei* using integrated analysis of the microbiome, transcriptome and metabolome. Ammonia and thermal stress caused variations in the intestinal bacterial community, with an increase in Firmicutes and a decrease in Bacteroidetes. The abundance of some beneficial substance-producing bacteria decreased, including *Formosa*, *Kriegella*, *Ruegeria*, *Rhodopirellula* and *Lutimonas*; pathogenic bacteria of the genus *Vibrio* increased under individual stress but decreased under combined stress. Genes were differentially expressed in the intestine, and the enriched pathways were involved in ABC transporter, amino acid, linoleic acid, and ascorbate and aldarate metabolism; the immune-related genes were associated with peritrophic membrane and antimicrobial processes. Dysfunction of haemolymph metabolism was also observed, and 10 metabolic markers were identified, including L-lactic acid, gulonic acid, docosahexaenoic acid, L-lysine, gamma-aminobutyric acid, methylmalonic acid, trans-cinnamate, *N*-acetylserotonin, adenine, and dihydrouracil. Several intestinal bacterial genera had significant correlations with host genes and metabolic markers, but their mechanisms still need to be explored.

CRedit authorship contribution statement

Y.D. designed and performed the experiments, data analyse, and wrote the manuscript. D.X. performed the experiments and data analyse. J.Z. assisted in the experimental design, and edited of the manuscript. Y.W., H.L., and H.D. contributed to the sampling and data analyse. All authors reviewed the final manuscript.

Declaration of competing interest

The authors declare that they have no known competing financial interests or personal relationships that could have appeared to influence the work reported in this paper.

Acknowledgments

This study was supported by the earmarked fund for the Central Public-interest Scientific Institution Basal Research Fund, South China Sea Fisheries Research Institute, CAFS (2019TS18, 2020XK03); National Natural Science Foundation of China (31902343); Guangzhou Rural Science and Technology Commissioner Project (GZKTP201813); Central Public-interest Scientific Institution Basal Research Fund, CAFS (2019CY0103); Guangdong Natural Science Foundation (2017A030313147, 2019A1515012159); Ministry of Agriculture and Rural Affairs Financial Special Project (NHYYSWZZZYKZX2020). The authors are grateful to the laboratory staff for technical assistance, especially for the microbiota and transcriptome analysis support by Mingke Biotechnology (Hangzhou) Co., Ltd., and metabolome analysis support by Suzhou BioNovoGene Biomedical Tech Co., LTD.

Appendix A. Supplementary data

Supplementary data to this article can be found online at <https://doi.org/10.1016/j.scitotenv.2020.141867>.

References

- Achbergerová, L., Nahálka, J., 2014. Degradation of polyphosphates by polyphosphate kinases from *Ruegeria pomeroyi*. *Biotechnol. Lett.* 36 (10), 2029–2035.
- Aguilar, V., Racotta, I.S., Goytortúa, E., Wille, M., Sorgeloos, P., Civera, R., et al., 2012. The influence of dietary arachidonic acid on the immune response and performance of Pacific whiteleg shrimp, *Litopenaeus vannamei*, at high stocking density. *Aquac. Nutr.* 18, 258–271.
- Apitanyasai, K., Amparyup, P., Charoensapsri, W., Senapin, S., Tassanakajon, A., 2015. Role of *Penaeus monodon* hemocyte homeostasis associated protein (PmHHAP) in regulation of caspase-mediated apoptosis. *Dev. Comp. Immunol.* 53, 234–243.
- Argayosa, A.M., Bernal, R.A.D., Luczon, A.U., Arboleda, J.S., 2011. Characterization of mannose-binding protein isolated from the African catfish (*Clarias gariepinus* B.) serum. *Aquaculture* 310, 274–280.
- Chen, J.C., Liu, P.C., Lin, Y.T., 1988. Super intensive culture of red-tailed shrimp *Penaeus penicillatus*. *J. World Aquacult. Soc.* 19, 127–131.
- Cheng, W., Chen, J.C., 2002. The virulence of *Enterococcus* to freshwater prawn *Macrobrachium rosenbergii* and its immune resistance under ammonia stress. *Fish Shellfish Immunol.* 12, 97–109.
- Cheng, W., Tsai, L.H., Huang, C.J., Chiang, P.C., Cheng, C.H., Yeh, M.S., 2008. Cloning and characterization of hemolymph clottable proteins of kuruma prawn (*Marsupenaeus japonicus*) and white shrimp (*Litopenaeus vannamei*). *Dev. Comp. Immunol.* 32, 265–274.
- Cottrell, M.T., Kirchman, D.L., 2000. Natural assemblages of marine proteobacteria and members of the *Cytophaga-Flavobacter* cluster consuming low- and high-molecular weight dissolved organic matter. *Appl. Environ. Microbiol.* 66 (4), 1692–1697.
- Currey, L.M., Heupel, M.R., Simpfendorfer, C.A., Clark, T.D., 2013. Blood lactate loads of redthroat emperor *Lethrinus miniatus* associated with angling stress and exhaustive exercise. *J. Fish Biol.* 83 (5), 1401–1406.
- Ding, Z., Zhou, J., Kong, Y., Zhang, Y., Cao, F., Luo, N., et al., 2018. Dietary arachidonic acid promotes growth, improves immunity, and regulates the expression of immune-related signaling molecules in *Macrobrachium nipponense* (De Haan). *Aquaculture* 484, 112–119.
- Dogs, M., Wemheuer, B., Wolter, L., Bergen, N., Daniel, R., Simon, M., et al., 2017. Rhodobacteraceae on the marine brown alga *Fucus spiralis* are abundant and show physiological adaptation to an epiphytic lifestyle. *Syst. Appl. Microbiol.* 40, 370–382.
- Downes, J., Dewhirst, F.E., Tanner, A.C.R., Wade, W.G., 2013. Description of *Alloprevotella rava* gen. nov., sp. nov., isolated from the human oral cavity, and reclassification of *Prevotella tannerae* Moore et al. 1994 as *Alloprevotella tannerae* gen. nov., comb. nov. *Int. J. Syst. Evol. Microbiol.* 63, 1214–1218.
- Du, X.J., Wang, J.X., Liu, N., Zhao, X.F., Li, F.H., Xiang, J.H., 2006. Identification and molecular characterization of a peritrophin-like protein from fleshy prawn (*Fenneropenaeus chinensis*). *Mol. Immunol.* 43 (10), 1633–1644.
- Duan, Y.F., Liu, Q.S., Zhang, J.S., Wang, Y., Xiong, D.L., 2018a. Impairment of the intestine barrier function in *Litopenaeus vannamei* exposed to ammonia and nitrite stress. *Fish Shellfish Immunol.* 78, 279–288.
- Duan, Y.F., Wang, Y., Zhang, J.S., Xiong, D.L., 2018b. Elevated temperature disrupts the mucosal structure and induces an immune response in the intestine of whiteleg shrimp *Litopenaeus vannamei* (Boone, 1931) (Decapoda: Dendrobranchiata: Penaeidae). *J. Crustac. Biol.* 38 (5), 635–640.
- Edgar, R.C., 2013. UPARSE: highly accurate OTU sequences from microbial amplicon reads. *Nat. Methods* 10, 996–998.
- Edgar, R.C., Haas, B.J., Clemente, J.C., Quince, C., Knight, R., 2011. UCHIME improves sensitivity and speed of chimera detection. *Bioinformatics* 27, 2194–2200.
- Fan, L.F., Wang, Z.L., Chen, M.S., Qu, Y.X., Li, J.Y., Zhou, A.G., et al., 2019. Microbiota comparison of Pacific white shrimp intestine and sediment at freshwater and marine cultured environment. *Sci. Total Environ.* 657, 1194–1204.
- Fu, S.Z., Fan, H.X., Liu, S.J., Liu, Y., Liu, Z.P., 2009. A bioaugmentation failure caused by phage infection and weak biofilm formation ability. *J. Environ. Sci.* 21, 1153–1161.
- Galat, A., 1993. Peptidylproline cis-trans-isomerases: immunophilins. *Eur. J. Biochem.* 216, 689–707.
- Gao, C., Fu, Q., Su, B., Zhou, S., Liu, F., Song, L., et al., 2016. Transcriptomic profiling revealed the signatures of intestinal barrier alteration and pathogen entry in turbot (*Scophthalmus maximus*) following *Vibrio anguillarum* challenge. *Dev. Comp. Immunol.* 65, 159–168.
- Gentile, C.L., Weir, T.L., 2018. The gut microbiota at the intersection of diet and human health. *Science* 362 (6416), 776–780.
- Gilliland, M.G., Young, V.B., Huffnagle, G.B., 2012. Chapter 40- gastrointestinal microbial ecology with perspectives on health and disease. In: Johnson, L.R., Ghishan, F.K., Kaunitz, J.D., Merchant, J.L., Said, H.M., Wood, J.D. (Eds.), *Physiology of the Gastrointestinal Tract*, Fifth edition Academic Press, Boston, pp. 1119–1134.
- Giri, I.N.A., Teshima, S., Kanazawa, A., Ishikawa, M., 1997. Effects of dietary pyridoxine and protein levels on growth, vitamin B6 content, and free amino acid profile of juvenile *Penaeus japonicus*. *Aquaculture* 157 (3–4), 263–275.
- Harpaz, S., 2005. L-Carnitine and its attributed functions in fish culture and nutrition- a review. *Aquaculture* 249, 3–21.
- Hewitt, D.R., Duncan, P.F., 2001. Effect of high water temperature on the survival, moulting and food consumption of *Penaeus (Marsupenaeus) japonicus* (Bate, 1888). *Aquac. Res.* 32, 305–313.
- Holt, C.C., Bass, D., Stentiford, G.D., van der Giezen, M., 2020. Understanding the role of the shrimp gut microbiome in health and disease. *J. Invertebr. Pathol.* <https://doi.org/10.1016/j.jip.2020.107387>.
- Hsiao, E.Y., McBride, S.W., Hsien, S., Sharon, G., Hyde, E.R., McCue, T., et al., 2013. Microbiota modulate behavioral and physiological abnormalities associated with neurodevelopmental disorders. *Cell* 155, 1451–1463.
- Jackson, C.J., Wang, Y.G., 1998. Modelling growth rate of *Penaeus monodon* Fabricius in intensively managed ponds: effects of temperature, pond age and stocking density. *Aquac. Res.* 29, 27–36.
- Jaskulak, M., Grobelak, A., Vandenbulcke, F., 2020. Effects of sewage sludge supplementation on heavy metal accumulation and the expression of ABC transporters in *Sinapis alba* L. during assisted phytoremediation of contaminated sites. *Ecotox. Environ. Safe.* 197, 110606.
- Jiang, G.J., Yu, R.C., Zhou, M.J., 2004. Modulatory effects of ammonia-N on the immune system of *Penaeus japonicus* to virulence of white spot syndrome virus. *Aquaculture* 241, 61–75.
- Kanayama, N., Kajiwar, Y., Goto, J., Maradny, E.E., Maehara, K., Andou, K., et al., 1995. Inactivation of interleukin-8 by aminopeptidase N (CD13). *J. Leukoc. Biol.* 57, 129–134.
- Karlsson, F.H., Ussery, D.W., Nielsen, J., Nookaew, I., 2011. A closer look at bacteroides: phylogenetic relationship and genomic implications of a life in the human gut. *Microb. Ecol.* 61 (3), 473–485.
- Khorattanakulchai, N., Amparyup, P., Tassanakajon, A., 2017. Binding of PmClipSP2 to microbial cell wall components and activation of the proPO-activating system in the black tiger shrimp *Penaeus monodon*. *Dev. Comp. Immunol.* 77, 38–45.
- Kir, M., Kumlu, M., Erol, O.T., 2004. Effects of temperature on acute toxicity of ammonia to *Penaeus semisulcatus* juveniles. *Aquaculture* 241, 479–489.
- Klase, G., Lee, S., Liang, S., Kim, J., Zo, Y.G., Lee, J., 2019. The microbiome and antibiotic resistance in integrated fishfarm water: implications of environmental public health. *Sci. Total Environ.* 649, 1491–1501.
- Klindworth, A., Richter, M., Richter-Heitmann, T., Wegner, C.E., Frank, C.S., Harder, J., et al., 2014. Permanent draft genome of *Rhodospirillum rubrum* SWK7. *Mar. Genomics* 13, 11–12.
- Koeth, R.A., Wang, Z., Levison, B.S., Buffa, J.A., Org, E., Sheehy, B.T., et al., 2013. Intestinal microbiota metabolism of L-carnitine, a nutrient in red meat, promotes atherosclerosis. *Nat. Med.* 19, 576–585.
- Lee, M.C., Park, J.C., Lee, J.S., 2018. Effects of environmental stressors on lipid metabolism in aquatic invertebrates. *Aquat. Toxicol.* 200, 83–92.
- Levy, M., Blacher, E., Elinav, E., 2017. Microbiome, metabolites and host immunity. *Curr. Opin. Microbiol.* 35, 8–15.
- Lin, Y.C., Chen, J.C., 2001. Acute toxicity of ammonia on *Litopenaeus vannamei* Boone juveniles at different salinity levels. *J. Exp. Mar. Biol. Ecol.* 259, 109–119.
- Liu, C.H., Chen, J.C., 2004. Effect of ammonia on the immune response of white shrimp *Litopenaeus vannamei* and its susceptibility to *Vibrio alginolyticus*. *Fish Shellfish Immunol.* 16, 321–334.

- Lynch, K.M., Mcsweeney, P.L.H., Arendt, E.K., Uniacke-Lowe, T., Galle, S., Coffey, A., 2014. Isolation and characterisation of exopolysaccharide producing *Weissella* and *Lactobacillus* and their application as adjunct cultures in Cheddar cheese. *Int. Dairy J.* 34 (1), 125–134.
- Mali, B., Mohrlen, F., Frohne, M., Frank, U., 2004. A putative double role of a chitinase in a cnidarian: pattern formation and immunity. *Dev. Comp. Immunol.* 28, 973–981.
- Maniatsi, S., Farmaki, T., Abatzopoulos, T.J., 2015. The study of fkbp and ubiquitin reveals interesting aspects of *Artemia* stress history. *Comp. Biochem. Physiol. B* 186, 8–19.
- Nedashkovskaya, O.I., Suzuki, M., Kim, S.B., Mikhailov, V.V., 2008. *Kriegella aquimaris* gen. nov., sp. nov., isolated from marine environments. *Int. J. Syst. Evol. Microbiol.* 58, 2624–2628.
- Nguyen, B.T., Koshio, S., Sakiyama, K., Harakawa, S., Gao, J., Mamaug, R.E., et al., 2012. Effects of dietary vitamins C and E and their interactions on reproductive performance, larval quality and tissue vitamin contents in kuruma shrimp, *Marsupenaeus japonicus* Bate. *Aquaculture* 334–337, 73–81.
- Ogata, S., Shimizu, K., Tominaga, S., Nakanishi, K., 2017. Immunohistochemical study of mucins in human intestinal spirochetosis. *Hum. Pathol.* 62, 126–133.
- O'Sullivan, L.A., Weightman, A.J., Fry, J.C., 2002. New degenerate *Cytophaga-Flexibacter-Bacteroides*-specific 16S ribosomal DNA-targeted oligonucleotide probes reveal high bacterial diversity in River Taff epilithon. *Appl. Environ. Microbiol.* 68 (1), 201–210.
- Park, J.H., Ahn, H.J., Kim, S.G., Chung, C.H., 2013. Dextran-like exopolysaccharide-producing *Leuconostoc* and *Weissella* from kimchi and its ingredients. *Food Sci. Biotechnol.* 22 (4), 1047–1053.
- Pörtner, H.O., Knust, R., 2007. Climate change affects marine fishes through the oxygen limitation of thermal tolerance. *Science* 315, 95–97.
- Preston, N.P., Burford, M.A., Jackson, C.J., Crocos, P.J., 1995. Sustainable shrimp farming in Australia - prospects and constraints. *Sustainable Aquaculture 95, Proceedings. PACON 95, Pacific Congress on Marine Science and Technology, Honolulu, HI, USA*, pp. 308–316.
- Proost, P., Mortier, A., Loos, T., Vandercappellen, J., Gouwy, M., Ronsse, I., et al., 2007. Proteolytic processing of CXCL11 by CD13/aminopeptidase N impairs CXCR3 and CXCR7 binding and signaling and reduces lymphocyte and endothelial cell migration. *Blood* 110, 37–44.
- Qiao, R., Sheng, C., Lu, Y., Zhang, Y., Ren, H., Lemos, B., 2019. Microplastics induce intestinal inflammation, oxidative stress, and disorders of metabolome and microbiome in zebrafish. *Sci. Total Environ.* 662, 246–253.
- Sangsuriya, P., Senapin, S., Huang, W.P., Lo, C.F., Flegel, T.W., 2011. Co-interactive DNA binding between a novel, immunophilin-like shrimp protein and VP15 nucleocapsid protein of white spot syndrome virus. *PLoS One* 6, e25420.
- Schloss, P.D., Gevers, D., Westcott, S.L., 2011. Reducing the effects of PCR amplification and sequencing artifacts on 16S rRNA-based studies. *PLoS One* 6 (12), e27310.
- Segata, N., Izard, J., Waldron, L., Gevers, D., Miropolsky, L., et al., 2011. Metagenomic biomarker discovery and explanation. *Genome Biol.* 12, R60.
- Shin, N.R., Whon, T.W., Bae, J.W., 2015. Proteobacteria: microbial signature of dysbiosis in gut microbiota. *Trends Biotechnol.* 33, 496–503.
- Silchenko, A.S., Rasin, A.B., Kusaykin, M.I., Malyarenko, O.S., Shevchenko, N.M., Zueva, A.O., et al., 2018. Modification of native fucoidan from *Fucus evanescens* by recombinant fucoidanase from marine bacteria *Formosa* algae. *Carbohydr. Polym.* 193, 189–195.
- Soto-Rodriguez, S.A., Gomez-Gil, B., Lozano-Olvera, R., Betancourt-Lozano, M., Morales-Covarrubias, M.S., 2015. Field and experimental evidence of *Vibrio parahaemolyticus* as the causative agent of acute hepatopancreatic necrosis disease of cultured shrimp (*Litopenaeus vannamei*) in northwestern Mexico. *Appl. Environ. Microbiol.* 81, 1689–1699.
- Stuss, M., Wiktorska, J.A., Sevalnek, E., Stuss, M., Wiktorska, J.A., Sewerynek, E., 2010. N-acetylserotonin reduces lipopolysaccharide-induced lipid peroxidation in vitro more effectively than melatonin. *Neuro Endocrinol. Lett.* 31 (4), 489–496.
- Tinkov, A.A., Gritsenko, V.A., Skalnaya, M.G., Cherkasov, S.V., Aaseth, J., Skalny, A.V., 2018. Gut as a target for cadmium toxicity. *Environ. Pollut.* 235, 429–434.
- Turnbaugh, P.J., Hamady, M., Yatsunenko, T., Cantarel, B.L., Duncan, A., Ley, R.E., et al., 2008. A core gut microbiome in obese and lean twins. *Nature* 457, 480.
- Wang, F.I., Chen, J.C., 2006. The immune response of tiger shrimp *Penaeus monodon* and its susceptibility to *Photobacterium damsela* subsp. *damsela* under temperature stress. *Aquaculture* 258, 34–41.
- Wei, H.W., Wang, L.H., Hassana, M., Xie, B., 2018. Succession of the functional microbial communities and the metabolic functions in maize straw composting process. *Bioresour. Technol.* 256, 333–341.
- Wexler, H.M., 2007. Bacteroides: the good, the bad, and the nitty-gritty. *Clin. Microbiol. Rev.* 20, 593–621.
- Wu, F., Liu, M., Chen, C., Chen, J., Tan, Q., 2016. Effects of dietary gamma-aminobutyric acid on growth performance, antioxidant status, and feeding-related gene expression of juvenile grass carp, *Ctenopharyngodon idellus*. *J. World Aquacult. Soc.* 47, 820–829.
- Xie, S.W., Li, Y.T., Zhou, W.W., Tian, L.X., Li, Y.M., Zeng, S.L., et al., 2015. Effect of γ -aminobutyric acid supplementation on growth performance, endocrine hormone and stress tolerance of juvenile Pacific white shrimp, *Litopenaeus vannamei*, fed low fishmeal diet. *Aquac. Nutr.* 23, 54–62.
- Yamaguchi, H., Arisaka, H., Seki, M., Adachi, M., Kimura, K., Tomaru, Y., 2016. Phosphotriesterase activity in marine bacteria of the genera *Phaeobacter*, *Ruegeria*, and *Talassospira*. *Int. Biodeterior. Biodegradation* 115, 186–191.
- Yang, W., Han, L., Mandlala, M., Zhang, H., Zhang, Z., Xu, H., 2017. A plate method for rapid screening of *Ketogulonigenium vulgare* mutants for enhanced 2-keto-l-gulononic acid production. *Braz. J. Microbiol.* 48 (3), 397–402.
- You, X.X., Su, Y.Q., Mao, Y., Liu, M., Wang, J., Zhang, M., Wu, C., 2010. Effect of high water temperature on mortality, immune response and viral replication of WSSV infected *Marsupenaeus japonicus* juveniles and adults. *Aquaculture* 305, 133–137.
- Zhang, J., Liu, Y., Tian, L., Yang, H., Liang, G., Xu, D., 2012. Effects of dietary mannan oligosaccharide on growth performance, gut morphology and stress tolerance of juvenile Pacific white shrimp, *Litopenaeus vannamei*. *Fish Shellfish Immunol.* 33, 1027–1032.
- Zhang, M., Chen, C., You, C., Chen, B., Wang, S., Li, Y., 2019. Effects of different dietary ratios of docosahexaenoic to eicosapentaenoic acid (DHA/EPA) on the growth, non-specific immune indices, tissue fatty acid compositions and expression of genes related to LC-PUFA biosynthesis in juvenile golden pompano *Trachinotus ovatus*. *Aquaculture* 505, 488–495.
- Zhou, Z.K., Gu, W.B., Wang, C., Zhou, Y.L., Tu, D.D., Liu, Z.P., et al., 2018. Seven transcripts from the chitinase gene family of the mud crab *Scylla paramamosain*: their expression profiles during development and moulting and under environmental stresses. *Aquac. Res.* 49 (10), 3296–3308.
- Zimmermann, M., Zimmermann-Kogadeeva, M., Wegmann, R., Goodman, A.L., 2019. Separating host and microbiome contributions to drug pharmacokinetics and toxicity. *Science* 363 (6427), eaat9931.